Journal of Power Sources 201 (2012) 136–141

Contents lists available at SciVerse ScienceDirect

Journal of Power Sources

journal homepage: www.elsevier.com/locate/jpowsour

Stainless steel mesh coated with MnO_2/carbon nanotube and polymethylphenyl siloxane as low-cost and high-performance microbial fuel cell cathode materials

Yanfeng Chen[a,b], Zhisheng Lv[a,b], Jianming Xu[a,b], Dongqing Peng[a,b], Yingxin Liu[a,b], Jiaxian Chen[a,b], Xibo Sun[a], Chunhua Feng[a,*], Chaohai Wei[a]

[a] The Key Lab of Pollution Control and Ecosystem Restoration in Industry Clusters, Ministry of Education, College of Environmental Science and Engineering, South China University of Technology, Guangzhou 510006, PR China
[b] College of Chemistry and Chemical Engineering, South China University of Technology, Guangzhou 510640, PR China

ARTICLE INFO

Article history:
Received 6 May 2011
Received in revised form 5 August 2011
Accepted 27 October 2011
Available online 12 November 2011

Keywords:
Microbial fuel cell
Manganese oxide
Carbon nanotube
Polymethylphenyl siloxane
Stainless steel mesh

ABSTRACT

The use of inexpensive and high-performance cathode materials is important for constructing large-scale microbial fuel cells (MFCs) for wastewater treatment and bioelectricity production. We show that the air-breathing MFC with a MnO_2 (68%)/CNT and polymethylphenyl siloxane (PMPS) coated-stainless steel mesh cathode delivers a maximum power density of 2676 mW m^{-2} (normalized to the cathode surface area) or 86 W m^{-3} (normalized to the anode chamber volume). The cathode performance is found to be highly replied on the percentage of MnO_2 in the as-prepared MnO_2/CNT nanocomposites, in which the birnessite-type MnO_2 is uniformly formed on the exterior CNT surfaces, as revealed by the scanning electron microscopy (SEM) and X-ray diffraction (XRD) results. Furthermore, it is found that PMPS coated onto the mesh electrode offers the advantages of low cost, easy handling and low water loss and exhibits improved cathode performance as compared to polydimethyl siloxane (PDMS). These findings suggest that the cathode materials, MnO_2/CNT and PMPS in MFCs can function well as the electrocatalysts and the water-repellent gas-diffusion layer, respectively.

1. Introduction

A microbial fuel cell (MFC) is a biological reactor for bioelectricity generation, in which bacteria help to oxidize organic matter and transfer electrons to the anode, and electrons pass through an external circuit and arrive at the cathode to react with electron-acceptors (i.e., oxygen). Air-breathing microbial fuel cells (MFCs), typically characterized by using natural convection air-flow to their cathodes, are attractive for wastewater treatment applications due to their simple single-chamber construction and their unique ability to remove organic matter and generate bioelectricity. The high cost of cathode materials represents one of the significant challenges for their large-scale applications, because it is estimated to account for 47% (this value can be further raised to 75% if the membrane is removed from the cells) of MFC capital costs [1]. Such high cost is caused by the use of expensive Pt electrocatalysts, carbon cloth/paper electrode, catalyst binders like Nafion and polytetrafluoroethylene (PTFE). This prompts a growing body of research [2–10] to seek cost-effective cathode materials that are essential for manufacturing MFC on a large scale. These inexpensive materials, however once integrated into cathodes, are expected to offer even better, or at least comparable performance compared to the traditionally used expensive counterparts.

Several research groups [9–14] have previously shown that non-precious MnO_2 electrocatalysts as alternatives to Pt used in MFCs were highly efficient for catalyzing oxygen reduction reaction (ORR) and at the same time lowering overall costs. For example, Li et al. [11,12] experimentally compared the performance of a MnO_2 MFC and a Pt MFC in terms of their energy output and ability to remove organic contaminant, concluding that MnO_2 with a cryptomelane-type octahedral molecular sieve structure and doped with Co performed better than commercial Pt due to the enhanced reaction rate of ORR. Recent studies [2–4] have also paid their attention towards development of air-breathing MFCs equipped with stainless steel mesh to replace carbon cloth as the cathode catalyst support, because this material is more conductive and adjustable in addition to its low cost. Zhang et al. [2] showed that a maximum power density of 1610 mW m^{-2} was achieved for the air-breathing MFC with its cathode constructed onto stainless steel mesh and coated with polydimethyl siloxane (PDMS, which functions as the water-repellent gas diffusion layer), comparable to 1635 mW m^{-2} obtained with a carbon cloth MFC. Similar results were reported in the work [3] also using stainless steel mesh as gas diffusion electrode but coated with PTFE.

* Corresponding author. Tel.: +86 20 39380502; fax: +86 20 39380588.
E-mail address: chfeng@scut.edu.cn (C. Feng).

0378-7753/$ – see front matter © 2011 Elsevier B.V. All rights reserved.
doi:10.1016/j.jpowsour.2011.10.134

These previous results accelerated development of MFCs for large-scale fabrication and pave the way for further cost reduction by using inexpensive cathode materials. In this contribution, we investigated the role of low-cost carbon nanotube (CNT) supported MnO_2 (MnO_2/CNT) electrocatalysts in enhancing the cathode performance and therefore the bioelectricity generation. Considerable reports [15–18] have demonstrated that low-cost carbon supported MnO_x nanoparticles exhibited remarkable catalytic activity for ORR occurring at the air-cathode of alkaline metal-air batteries and alkaline fuel cells. Here, CNT was selected as the cathode material thanks to their advantages of large surface area, good conductivity and superior electrochemical activity [19]. Furthermore, we examined the use of polymethylphenyl siloxane (PMPS) coated onto the stainless steel mesh to serve as the water-repellent gas diffusion layer. In comparison with PDMS, PMPS not only possesses the water-proof property induced by the presence of methyl groups, but also offers better stability and adhesion due to the introduction of phenyl groups that provides steric hindrance towards chain motion [20].

In order to experimentally verify the feasibility and efficacy of using MnO_2/CNT and PMPS as low-cost and high-performance MFC cathode materials, we constructed a series of air-breathing cathodes onto stainless steel mesh combined with coatings of these materials and compared their cell performance with that obtained from benchmark MFCs. The MnO_2/CNT electrocatalysts were prepared by a direct redox reaction of CNT with $KMnO_4$ at a controlled pH and characterized by scanning electron microscopy (SEM) and X-ray diffraction (XRD) techniques. Because the catalytic activity of carbon supported MnO_x nanoparticles for ORR was highly sensitive to the percentage of MnO_x in the carbon material and its crystal structure [18], we also examined the effect of catalyst composition on MFC performance.

2. Materials and methods

2.1. Synthesis and characterizations of MnO_2/CNT composites

CNTs with a diameter of 10–20 nm and a length of 5–15 μm (Shenzhen NanoHarbo Co., China) were used as the catalyst supports. The preparation of CNT supported MnO_2 nanocomposites were conducted by a direct redox reaction between the CNTs and $KMnO_4$, according to the procedures described in the literature [21,22]. First, a $KMnO_4$ solution having a total volume of 200 mL was preheated to 70 °C. Then, 1.0 g of the CNTs were added to the hot $KMnO_4$ solution and left to react with stirring and at a controlled temperature of 70 °C. The pH of the reaction solution was controlled at 1.0 by adding 2 M HCl solution. Different MnO_2/CNT samples varying in the percentage of MnO_2 in the composite were obtained using different concentrations of $KMnO_4$ solution in the range from 0.01 to 0.1 M. After 6-h reaction, the complete disappearance of the violet color of MnO_4^- was observed in all samples. The resulting colorless suspension was then filtered, washed several times with distilled water until the pH approached 7.0, and dried at 100 °C for 12 h in a vacuum oven. Assuming that MnO_4^- was completely reduced to MnO_2 in all cases, we can obtain the desired MnO_2/CNT composites containing 15%, 30%, 45%, 60% and 68% of MnO_2, in relation to the initial $KMnO_4$ solution of 0.01, 0.025, 0.045, 0.075 and 0.10 M, respectively. It should be noted that when the concentration of $KMnO_4$ solution exceeded 0.10 M, incomplete reaction between the CNTs and $KMnO_4$ occurred, as evidenced from the observation of violet solution even when the reaction time lasted for 12 h.

The surface morphologies of the unmodified CNTs and the as-prepared MnO_2/CNT composites varying in the percentage of MnO_2 were examined by a LEO 1530 VP scanning electron microscope. The powder X-ray diffraction (XRD) patterns of these materials were recorded on a Bruker D8 Advance X-ray diffractometer with Cu Ka radiation (1.54178 Å).

2.2. Electrochemical characterization using a rotating disk electrode (RDE)

A glassy carbon (GC) disk electrode with a diameter of 3 mm was used as the RDE on which a thin catalyst layer was coated to form the catalyst-modified electrode. Prior to use, the bare GC electrode was first polished with emery paper and then with Al_2O_3 powders (particle sizes of 1 and 0.06 μm). The polished electrode was successively cleaned with ethanol and distilled water in an ultrasonic bath for 10 min, respectively. The catalyst-modified RDE was prepared as follows. A catalyst ink containing 5 mg of catalyst was prepared in a dilute Nafion solution (0.5 wt%, 250 μL, diluted by 2-propanol) ultrasonically for 20 min. Aliquots (2 μL) of the ink was then pipetted onto the electrode surface using a micro-syringe to form a thin catalyst layer. After air-drying for 30 min to evaporate the solvent, the RDE was transferred into the three-electrode electrochemical cell for measurements. The linear scanning voltammetry (LSV) tests were performed at room temperature in 0.1 M Na_2SO_4 solution using the prepared RDE as the working electrode, a platinum spiral as the counter electrode and a saturated calomel electrode (SCE) as the reference electrode. If not mentioned otherwise, all the reported voltages were referred to SCE. Before each test, the solution was bubbled with O_2 (99.999%) for 20 min to obtain the O_2-saturated environment. Voltammograms were recorded from 0.3 to −0.6 V with a scan rate of 10 mV s^{-1}.

2.3. Cathode preparation

A series of cathodes were prepared based on a conductive current collector, stainless steel mesh, onto which PMPS and MnO_2/CNT composites were added to function as water-repellent gas diffusion layer and catalyst layer, respectively. The stainless steel mesh (opening size of 104 μm; wire diameter of 66 μm; open area ratio of 37%; thickness of 135 μm) was purchased from Anping County Resen Screen Co., Ltd. (China). Prior to use, it was ultrasonically cleaned and degreased in acetone and ethanol successively each for 10 min, followed by rinsing with distilled water. PMPS (10 mg cm^{-2}) purchased from Guangzhou XSJ Co., Ltd. (China) was mixed with carbon black (2.4 mg cm^{-2}) to form a slurry. The slurry was then painted on one side of the stainless steel mesh that faced the air. The PDMS layer was allowed to be dried at room temperature for 30 min. Subsequently, the MnO_2/CNT electrocatalysts having different content of MnO_2 were coated on the other side of the stainless steel mesh that faced the anode solution. Before coating, the catalyst slurry was prepared by mixing 8.0 mg cm^{-2} MnO_2/CNT composites with 24.2 μL cm^{-2} 5 wt% Nafion (catalyst binder and proton conductor). In benchmarking performance of these cathodes, a control cathode was also prepared using PMPS and 5% Pt/C catalyst (5 mg cm^{-2}, Johnson Matthey). For all the cathodes, the projected cathode surface area was 2.4 cm × 3.3 cm.

2.4. MFC construction, operation and tests

Air-breathing membraneless MFCs consisting of a cathode described above and an anode were constructed with a rectangular anode chamber (made of polycarbonate) having an effective volume of 25 mL. The anode used for these MFC reactors was a piece of PPy/AQDS (anthraquinone-2,6-disulphonic disodium salt)-modified carbon felt (2.2 cm × 2.3 cm × 0.5 cm) prepared according to the procedures described previously [23,24]. All MFCs were inoculated with Shewanella decolorationis S12 bacteria which were

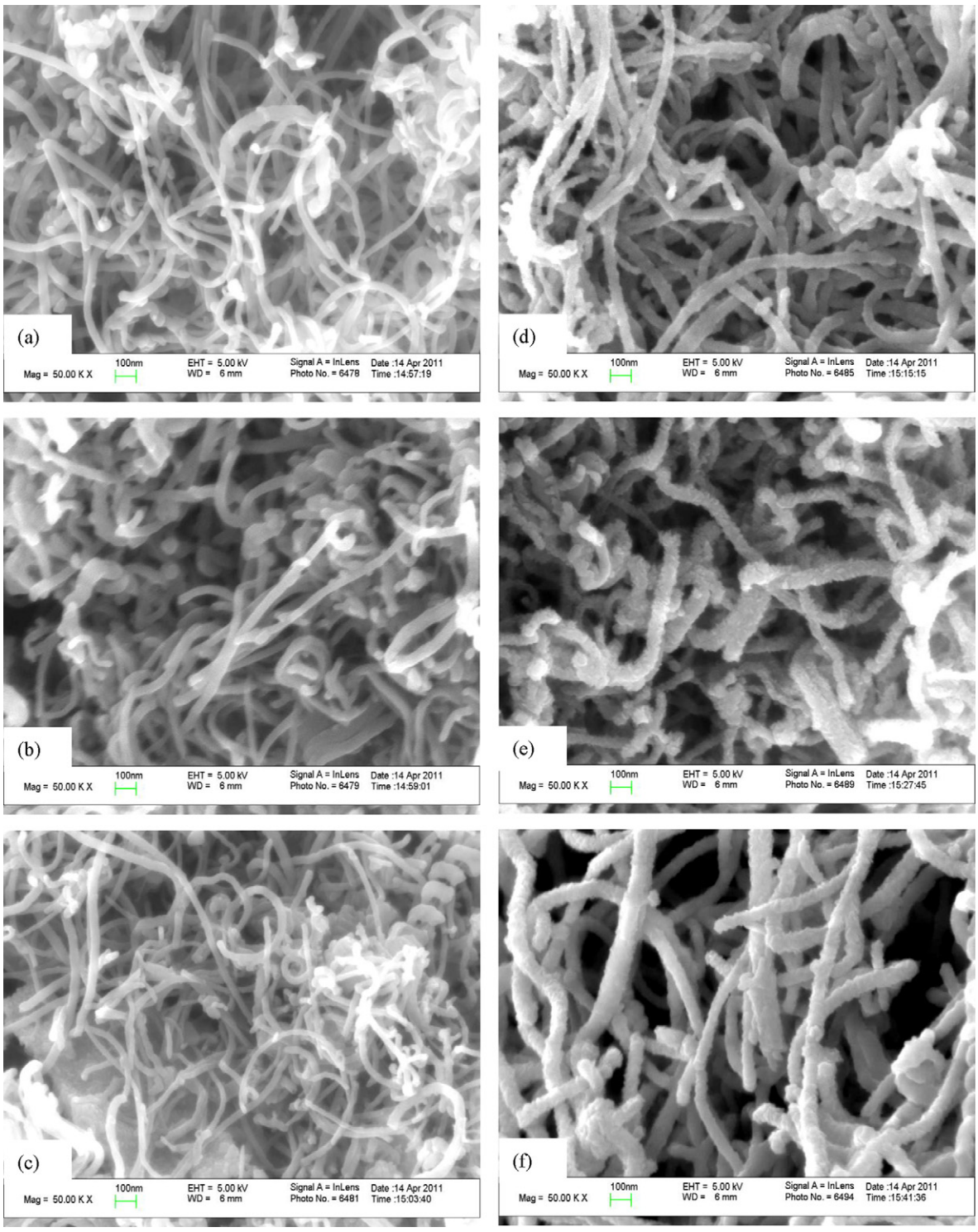

Fig. 1. SEM images of (a) unmodified CNTs, and (b)–(f) as-prepared MnO_2/CNT composites having the content of MnO_2 of 15%, 30%, 45%, 60%, 68%, respectively.

grown on the lactate-growth medium including 10 mM lactate and 0.1 M PBS-based nutrient solution (pH 8.0) consisting of 5.84 g L^{-1} NaCl, 0.10 g L^{-1} KCl, 0.25 g L^{-1} NH_4Cl, 10 mL of vitamin solution and 10 mL of mineral solution.

All MFCs were operated at a controlled temperature of 30 °C. A 32-channel voltage collection instrument (AD8223, China) was used to record the cell voltages under the conditions of a 1000 Ω external resistance. To evaluate power performance of MFCs, the anode and cathode polarization curves and the cell power density curves were obtained by varying the external resistor over the range from 10 to 8000 Ω when the performance of MFC approached steady state. Current density (I) was calculated as $I = V$ (cell voltage)/R (external resistance), and power density (P) was calculated as $P = V \times I$. Both I and P were normalized to the projected area of cathode surface. The anode potential was measured by inserting a sterilized SCE electrode into the anode chamber; the cathode potential was calculated as the sum of the anode potential and the cell voltage.

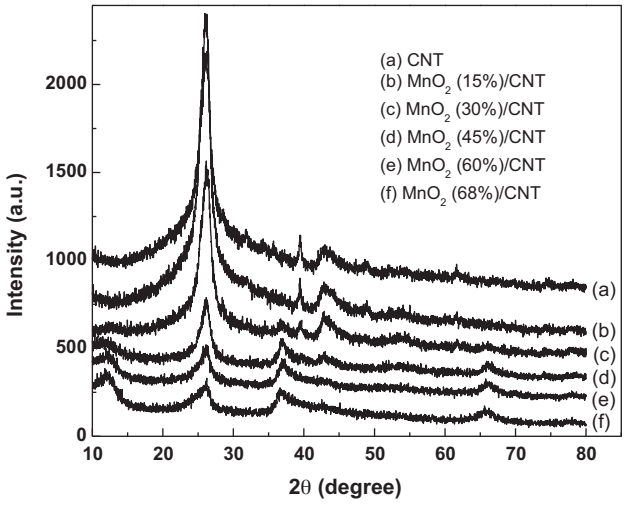

Fig. 2. Typical XRD patterns for unmodified CNTs and as-prepared MnO_2/CNT composites.

3. Results and discussion

3.1. Physicochemical characterizations of MnO_2/CNT electrocatalysts

A facile preparation method was employed for the synthesis of MnO_2/CNT electrocatalysts by the direct reaction between the CNTs and $KMnO_4$. Fig. 1 shows the typical top-view SEM images of the as-prepared MnO_2/CNT composites varying in the percentage of MnO_2 from 0 to 68%. The unmodified CNT composites have a porous network structure, consisting of CNTs with approximately 10–20 nm in diameter (Fig. 1a). Upon reaction with $KMnO_4$, the CNTs were uniformly decorated with MnO_2 particles on their surfaces. The incorporation of low percentages of MnO_2 in the CNTs, however, did not lead to significant changes in the morphologies of CNTs (Fig. 1a–c). In contrast, Fig. 1d clearly shows that a thin layer composing of MnO_2 was homogeneously deposited on the CNT surfaces, as evidenced from the increased thickness of tubes. Furthermore, Fig. 1d–f illustrates that increasing the content of MnO_2 from 45% to 68% resulted in the increasing tube diameter and surface roughness, suggesting the homogeneous growth of MnO_2. It was noted that there was no agglomeration of MnO_2 on the exterior CNT surfaces; that is, the coatings of MnO_2 did not change the overall porous structure of CNTs. These features suggest that the as-prepared MnO_2/CNT electrocatalysts have a promising network nanostructure for catalyzing ORR, as the nano-sized MnO_2 can be fully approached by oxygen.

The crystal structures of the synthetic MnO_2/CNT composites were examined by XRD characterization. Comparisons of XRD patterns among different samples (Fig. 2) revealed that the typical peaks at around 26°, 40°, 43° and 54° were attributable to the CNTs and that the incorporation of MnO_2 on the CNTs caused a decrease in the height of these peaks. The appearance of peaks at 12°, 37° and 66° was resulted from the presence of MnO_2. In agreement with previous reports [21], these peaks are indicative of the formation of birnessite-type MnO_2 on the CNT surfaces.

3.2. Power performance of air-breathing MFCs equipped with MnO_2/CNT electrocatalysts

In order to verify and explore the effects of CNT–MnO_2 composition on the ORR activity in MFCs, a series of power density measurements were performed using the same cell architecture and anode system but a variety of cathode systems having different

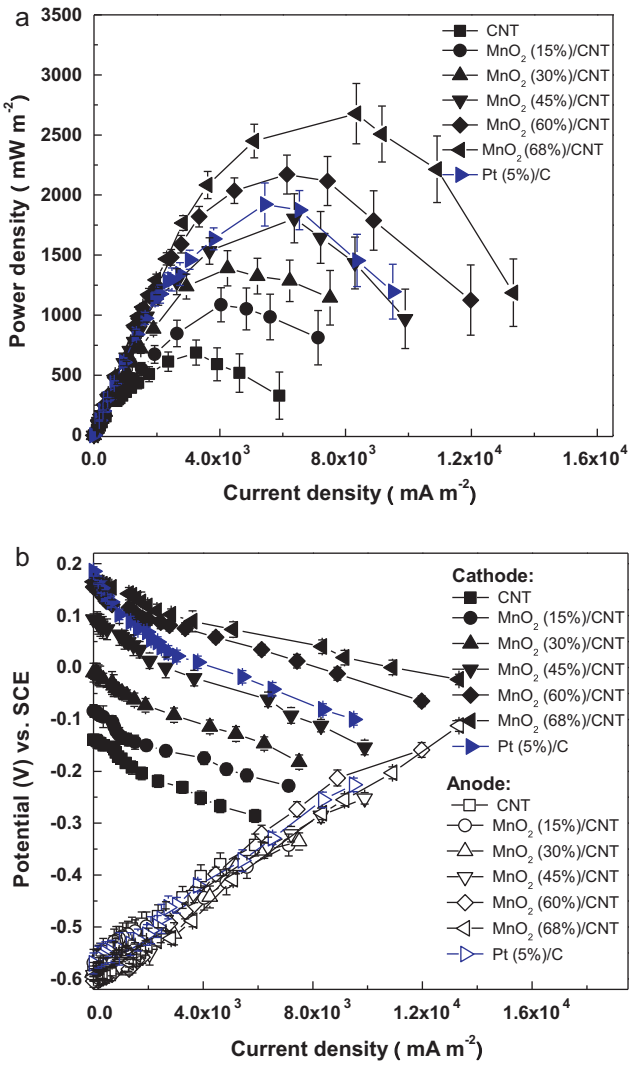

Fig. 3. (a) Power density curves, and (b) anode and cathode polarization curves of six air-breathing MFCs with stainless steel mesh cathodes coated with PMPS and MnO_2/CNT electrocatalysts varying in different MnO_2 contents. For comparison, such curves were also recorded for a benchmark Pt/C MFC having the same cell architecture and anode system. The data point shown represents the average on triplicate measurements obtained from three independent experiments ± standards deviations.

catalyst compositions. The power performance of MFC with Pt/C electrocatalysts was also tested for comparison. In all cases, the stainless steel mesh functioned as the cathode current collector, which was coated with PMPS on one side that faced air and cathode catalysts on the other side that faced the anode solution.

The results of these measurements are provided in Fig. 3a. It was noticeable that the content of MnO_2 in the catalyst can significantly affect the power performance. The MFC with the unmodified-CNT cathode produced a maximum power density of 688 mW m^{-2} (the surface area was referred to the projected cathode surface area throughout this study). Increasing the percentage of MnO_2 from 0 to 68% can substantially enhance the maximum power density. The decoration of CNT with 45% MnO_2 increased power by 2.6 times compared to the unmodified-CNT cathode. With an increase in the percentage of MnO_2 from 45% to 68%, the maximum power density increased from 1806 to 2676 mW m^{-2}. These observations indicate that the maximum power density trend was consistent with an overall increase in the amount of MnO_2 deposited on the CNT surfaces as revealed by the SEM results (Fig. 1). The benchmark Pt/C MFC generated a maximum power density of 1922 mW m^{-2}, which

was slightly larger than 1635 mW m^{-2} obtained from a similar MFC design [2] using carbon cloth cathode with Pt electrocatalysts and PDMS layers, but approximately 1.4 times less than the largest maximum power density achieved with the MnO_2 (68%)/CNT electrocatalysts.

To the best of our knowledge, the maximum power density of 2676 mW m^{-2}, equivalent to 86 W m^{-3} (the volume was referred to the anode chamber volume throughout this study) obtained from the MnO_2 (68%)/CNT-coated stainless steel mesh cathode, represents one of the best power densities ever reported for an air-breathing membraneless MFC design either using Pt or non-precious catalysts. For example, a stainless steel mesh cathode with PDMS and Pt achieved a maximum power density of 1610 mW m^{-2} (47 W m^{-3}) for the membraneless MFC [2]. When Pt was replaced by active carbon, this MFC delivered a maximum power density of 1220 mW m^{-2} (36 W m^{-3}) [4]. In addition, the best performance achieved here was significantly larger than that obtained from other works also using MnO_x particles as the cathode electrocatalysts but with different types of MnO_x and different cell designs. For example, nano-structured MnO_x particles electrodeposited on carbon paper were reported to be used as electrocatalysts for ORR in a continuous-mode air-breathing MFC, from which a maximum power density of 773 mW m^{-3} was obtained [13]. Zhang et al. [10] showed that the use of commercial MnO_2 electrocatalysts in conjunction with a canvas cloth cathode assembly produced a maximum power density of 86 mW m^{-2} (9.87 W m^{-3}) for a tubular air-cathode MFC. A recent report by Li et al. [11] revealed that Co-doped cryptomelane-type MnO_2 as the ORR electrocatalyst exhibited a maximum power density of 897 mW m^{-2} for a single-chamber air-cathode MFC. The substantially increased power performance in this study compared to other reports is believed to be the consequence of the remarkable electrocatalytic activity of MnO_2/CNT for ORR. This may be resulted from (i) the network porous nanostructure that facilitates oxygen transport in the catalysts and (ii) the uniform dispersion of nano-sized MnO_2 catalysts on the CNT supports, which provides a large available surface area for oxygen access.

The fact that the enhancement of cathode performance was mainly responsible for the boost of power performance was confirmed by the anode and cathode polarization curves (Fig. 3b). It was clear from the anode polarization curves that there were insignificant variations in the anode open circuit potentials (OCPs) and anode working potentials for all MFCs using MnO_2/CNT or Pt electrocatalysts. In contrast, the variations in the cathode OCPs and cathode working potentials were pronounced depending on the percentage of MnO_2 and the type of catalysts. It was proposed that the successive two-electron ORR pathway is favored on carbon supported MnO_x electrocatalysts, as MnO_x mainly functions as the catalyst for the two-electron decomposition of hydrogen peroxide, which may be formed as the result of two-electron reduction of oxygen by the carbon electrode [17,18]. The low percentages of MnO_2 contained in the catalysts seemed to be ineffective for catalyzing hydrogen peroxide decomposition [18]; that is, the two-electron reduction of oxygen to hydrogen peroxide was dominant in these situations, thus causing the low cathode OCPs observed. The cathodes containing sufficiently high amount of MnO_2 turned to make ORR follow a four-electron reduction pathway, thus leading to the high cathode OCPs which were approximate to the value in relation to Pt. The slope of the cathode polarization curve indicates the magnitude of driving force (in the form of overpotential) required for the cathode reaction. Comparisons among different cathode polarization curves associated with MnO_2 (45%)/CNT, MnO_2 (60%)/CNT, MnO_2 (68%)/CNT and Pt (5%)/C catalysts suggested that the MnO_2 (68%)/CNT cathode exhibited the lowest slopes corresponding to the lowest overpotentials for driving the cathode reaction. This

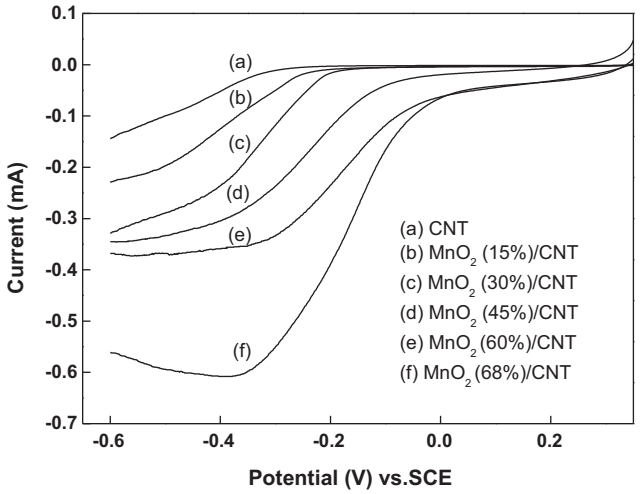

Fig. 4. LSV curves of the MnO_2/CNT electrocatalysts with different MnO_2 contents in 0.1 M Na2SO4 solution saturated with oxygen. The rotating speed was 2500 rpm.

accounts for the observation that the air-breathing MFC with the MnO_2 (68%)/CNT cathode performed best among all MFC tests.

RDE-based LSV tests were performed to provide evidence for the different ORR activities of the synthesized MnO_2/CNT catalysts. Fig. 4 shows the voltammograms of ORR recorded on RDEs modified with different MnO_2/CNT samples. It was clearly visible that both the onset potential of ORR and the ORR current varied substantially depending on the concentration of MnO_2 in the catalyst. Increasing the content of MnO_2 led to a positive shift of the onset potential and an increase in the reduction current. The RDE with MnO_2 (68%)/CNT exhibited the most positive onset potential and the highest limiting current among all the electrodes. These observations suggest that the activity of these catalysts increases in the order of CNT < MnO_2 (15%)/CNT < MnO_2 (30%)/CNT < MnO_2 (45%)/CNT < MnO_2 (60%)/CNT < MnO_2 (68%)/CNT.

The differences in ORR activity among the prepared MnO_2/CNT catalysts can also be evaluated from the Koutecky–Levich curves (Fig. 5) according to the following equation that has been widely used to analyze the ORR kinetics [17,25].

$$\frac{1}{i} = \frac{1}{i_k} + \frac{1}{i_d} = \frac{1}{nFAkC^0} - \frac{1}{0.62nFAD_{O_2}^{2/3}\nu^{-1/6}C^0\omega^{1/2}}$$

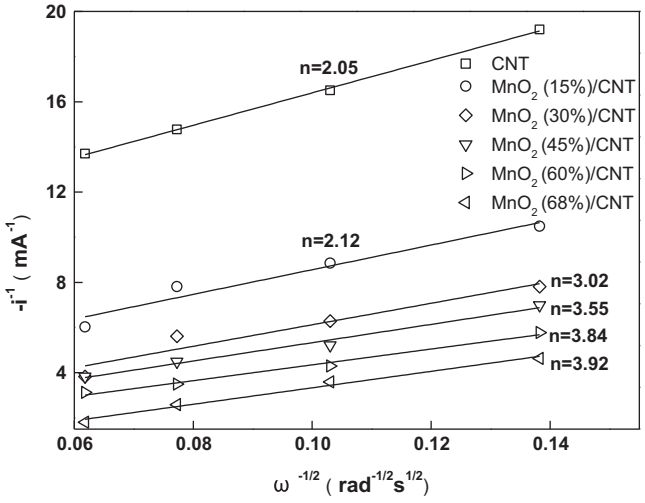

Fig. 5. Koutecky–Levich plots of ORR for the MnO_2/CNT electrocatalysts with different MnO_2 contents in 0.1 M Na_2SO_4 solution saturated with oxygen.

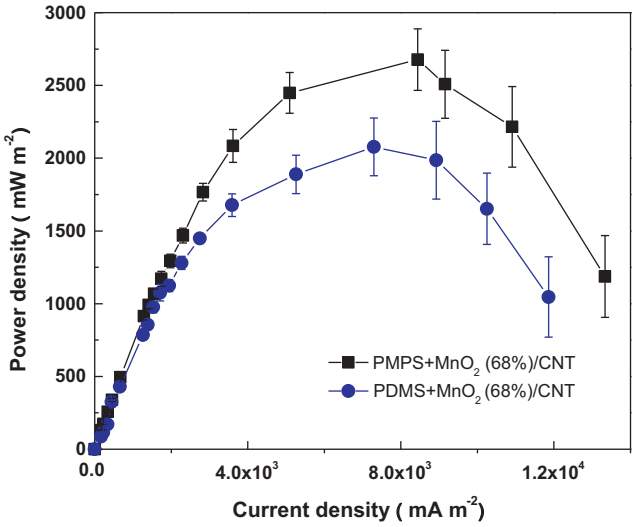

Fig. 6. Power density comparison between a PDMS MFC and a PMPS MFC. The data point shown represents the average on triplicate measurements obtained from three independent experiments ± standards deviations.

where i, i_k, and i_d are the measured, kinetic, and diffusion-limiting current, respectively; n is the number of electrons involved in ORR; F is the Faraday constant; A is the geometric electrode area; k is the rate constant for ORR; C^0 is the saturated concentration of oxygen in the electrolyte; D_{O_2} is the diffusion coefficient oxygen; ν is the kinetic viscosity of solution, and ω is the rotation rate. The n values calculated from the slopes of these curves were 2.05, 2.12, 3.02, 3.55, 3.84, and 3.92 for CNT, MnO_2 (15%)/CNT, MnO_2 (30%)/CNT, MnO_2 (45%)/CNT, MnO_2 (60%)/CNT, and MnO_2 (68%)/CNT, respectively. These results confirm that the pathway of ORR changes from two-electron reduction to four-electron reduction with the increasing content of MnO_2.

3.3. PMPS as an efficient water-repellent gas-diffusion layer in air-breathing MFCs

PDMS was recognized as an air-cathode material capable of allowing gas permeation from atmosphere to the catalyst active sites, and preventing water leakage from the cathode. Although very reactive, the limiting factor of PDMS used in MFCs is the relatively complex fabrication approach which requires additional silicone elastomer curing agent and high temperature for cross-linking the PDMS oligomers [2]. The approach of coating PMPS on the mesh electrode, however, appeared much more convenient as compared with that associated with PDMS, since PMPS can be assembled onto the electrode at room temperature eliminating the use of other curing agents and only 30-min curing time was required. The presence of phenyl groups in PMPS may account for its self-drying property.

Two separate MFC reactors were constructed, with one rector using the PMPS-based cathode and the other using PDMS-based cathode. Fig. 6 shows that the PDMS cathode containing the same amount of MnO_2 (68%)/CNT electrocatalysts produced a maximum power density of 2078 mW m^{-2}, decreased by 22% as compared to 2676 mW m^{-2} obtained from PMPS. In addition, for long-term MFC operations, it is necessary to control water loss from the cathode. It was found that PMPS was very effective in preventing water leakage, with around 5% loss for 1-week operation. This value was significantly lower than that (5% loss each day) in relation to PDMS cathode as reported elsewhere [2]. Taking into account the fact that it is a very low-cost (about 6$ kg^{-1}) material, in combination with all the advantages it provides, PMPS represents a promising potential material for large-scale construction of air-breathing MFCs.

4. Conclusions

We have experimentally demonstrated that the air-breathing MFC equipped with the MnO_2/CNT nanocomposites and PMPS-coated stainless steel mesh cathode delivered appreciably higher power density than that ever reported for a single-chamber MFC design. The use of MnO_2/CNT and PMPS showed advantages over other reported cathode materials such as Pt/C and PDMS in terms of their much lower cost and higher cathode performance. These advantages enable them to be employed as promising cathode materials for constructing large-scale MFCs for wastewater treatment and bioelectricity production. However, it should be noted that there are still several steps before their practical applications. One of the main concerns relates to the long-term stability of these materials used in MFCs, which will be explored in the future work.

Acknowledgements

We gratefully acknowledge financial support from the National Natural Science Foundation of China (Nos. 20803025, 21037001, 30800796), the Fundamental Research Funds for the Central Universities, SCUT (No. 2009ZM0026), the Innovation Experiment Program for University Students in Guangdong Province (No. S1010561057), and the Student Research Program of SCUT.

References

[1] R.A. Rozendal, H.V.M. Hamelers, K. Rabaey, J. Keller, C.J.N. Buisman, Trends Biotechnol. 26 (2008) 450–459.
[2] F. Zhang, T. Saito, S.A. Cheng, M.A. Hickner, B.E. Logan, Environ. Sci. Technol. 44 (2010) 1490–1495.
[3] S.J. You, X.H. Wang, J.N. Zhang, J.Y. Wang, N.Q. Ren, X.B. Gong, Biosens. Bioelectron. 26 (2011) 2142–2146.
[4] F. Zhang, S.A. Cheng, D. Pant, G.V. Bogaert, B.E. Logan, Electrochem. Commun. 11 (2009) 2177–2179.
[5] F. Zhao, F. Harnisch, U. Schröder, F. Scholz, P. Bogdanoff, I. Herrmann, Electrochem. Commun. 7 (2005) 1405–1410.
[6] N. Duteanu, B. Erable, S.M.S. Kumar, M.M. Ghangrekar, K. Scott, Bioresour. Technol. 101 (2010) 5250–5255.
[7] C.H. Feng, Q.Y. Wan, Z.S. Lv, X.J. Yue, Y.F. Chen, C.H. Wei, Biosens. Bioelectron. 26 (2011) 3953–3957.
[8] Y. Yuan, S.G. Zhou, L. Zhuang, J. Power Sources 195 (2010) 3490–3493.
[9] L.X. Zhang, C.S. Liu, L. Zhuang, W.S. Li, S.G. Zhou, J.T. Zhang, Biosens. Bioelectron. 24 (2009) 2825–2829.
[10] L. Zhuang, S.G. Zhou, Y.Q. Wang, C.S. Liu, S. Geng, Biosens. Bioelectron. 24 (2009) 3652–3656.
[11] X. Li, B. Hu, S. Suib, Y. Lei, B. Li, Biochem. Eng. J. 54 (2011) 10–15.
[12] X. Li, B. Hu, S. Suib, Y. Lei, B. Li, J. Power Sources 195 (2010) 2586–2591.
[13] X.W. Liu, X.F. Sun, Y.X. Huang, G.P. Sheng, K. Zhou, R.J. Zeng, F. Dong, S.G. Wang, A.W. Xu, Z.H. Tong, H.Q. Yu, Water Res. 44 (2010) 5298–5305.
[14] I. Roche, K. Katuri, K. Scott, J. Appl. Electrochem. 40 (2010) 13–21.
[15] I. Roche, K. Scott, J. Appl. Electrochem. 39 (2009) 197–204.
[16] A.C. Garcia, A.D. Herrera, E.A. Ticianelli, M. Chatenet, C. Poinsignon, J. Electrochem. Soc. 158 (2011) B290–B296.
[17] W. Sun, A. Hsu, R.R. Chen, J. Power Sources 196 (2011) 627–635.
[18] N. Ominde, N. Bartlett, X.Q. Yang, D.Y. Qu, J. Power Sources 195 (2010) 3984–3989.
[19] X.W. Zhang, J.L. Fu, Y. Zhang, L.C. Lei, Sep. Purif. Technol. 64 (2008) 116–123.
[20] P. Jha, L.W. Mason, J.D. Way, J. Membrane Sci. 272 (2006) 125–136.
[21] S.B. Ma, K.Y. Ahn, E.S. Lee, K.H. Oh, K.B. Kim, Carbon 45 (2007) 375–382.
[22] S.B. Ma, K.W. Nam, W.S. Yoon, X.Q. Yang, K.Y. Ahn, K.H. Oh, K.B. Kim, J. Power Sources 178 (2008) 483–489.
[23] C.H. Feng, L. Ma, F.B. Li, H.J. Mai, X.M. Lang, S.S. Fan, Biosens. Bioelectron. 25 (2010) 1516–1520.
[24] C.H. Feng, F.B. Li, H.Y. Liu, X.M. Lang, S.S. Fan, Electrochim. Acta 55 (2010) 2048–2054.
[25] F.Y. Cheng, Y. Su, J. Liang, Z.L. Tao, J. Chen, Chem. Mater. 22 (2010) 898–905.